

Design and Fabrication of a Metallic MEMS Gripper Using Electro-thermal V-shape and Modified U-shape Actuators

Jay J. Khazaai, H. Qu, M. Shillor, L. Smith, Ka. C. Cheok

Oakland University, Rochester, MI, USA
jkhazaai@oakland.edu

ABSTRACT

This paper reports the design, fabrication, and characterization of a distinctive MEMS gripper electro-thermally driven jointly by a new metallic V-shape actuator (VSA) and a set of modified Guckel U-shape actuators (mUSA). The modification of the angle ($90^\circ \pm \theta$) between the hot and cold arms in the mUSA facilitates desired unidirectional in-plane displacement and thus increases the opening of the gripper. A tip opening up to $173 \mu\text{m}$ has been measured within the operating voltage range. This unique configuration distinguishes this MEMS gripper from others in the capability of generation of larger tip displacement and greater holding force. The metallic structures allow a low operating voltage and low overall power consumption. MetalMUMPs is employed to fabricate the device, in which electroplated nickel is used as the structural material.

Keywords: MEMS, Micro Gripper, Micro Actuator, Electro-thermal, MetalMUMPs.

1 INTRODUCTION

MEMS grippers, when opening, require large mechanical driving force and displacement. The actuators used in driving the moving parts of the MEMS gripper shall generate a controllable and stable displacement with desired force in a guided direction. MEMS actuators responding to electrical signal within their transduction systems mainly fall into four classes [1] i.e., electrostatic, piezoelectric, electro-thermal, and electromagnetic. Electrostatic actuators suffer from less functional robustness and small range of controllable displacement. Electromagnetic and piezoelectric actuators have fabrication process complexities and material unavailability issues. The electro-thermal actuators have been more widely used due to the compatibility with standard IC fabrication process and materials; the capability in generating relatively large actuation displacement and force; and structural and functional robustness.

Previously, the authors have reported the design and fabrication of polysilicon switches consisting of similar V-shape and modified U-shape actuators [2-3]. Despite of the large displacement generated by the demonstrated polysilicon VSA and mUSA compared to other structures [4-5], in general, the achieved displacement of the polysilicon actuators may still be insufficient for MEMS

grippers where quite large traveling distance (tens of μm) and force (range of mN) are normally needed. This is mainly due to the relatively smaller thermal expansion coefficient of polysilicon than many metals. In design of the MEMS gripper with large opening, we have used electroplated nickel as the structural material for its larger thermal expansion coefficient and thus possible large desired displacement with limited device size. MetalMUMPs foundry service is used for the device fabrication. Critical design requirements such as large in-plane controllable actuator displacement and force in a guided direction, faster (re)initialization of the mechanical structure for faster (de)actuation, reliable alignment of the gripper tips, and minimized out-of-plane and rotational displacements of the structure are considered in the design. It should be noted that the unique VSA designed in this device is versatile and can be widely used as mechanical drivers in a variety of MEMS/BioMEMS devices, such as manipulators, switches, surgical instruments, and needles.

2 DESIGN OF GRIPPER ACTUATORS

Fig. 1 illustrates the structure of the designed metallic gripper in which a 4-arm VSA and two 2-arm mUSAs are employed. In operation, the simultaneous driving of the three actuators allows for superposition of forces generated by the VSA and mUSAs respectively and thus a greatly amplified desired tip displacement in x -direction. Fig. 2 (a) and (b) depict the mechanical structures of the metallic VSA and the mUSA used in the gripper shown in Fig. 1. The VSA provides the adequate mechanical pushing force, and the mUSA generates the guided in-plane opening and holding force at the gripper tips. As presented in [2-3],

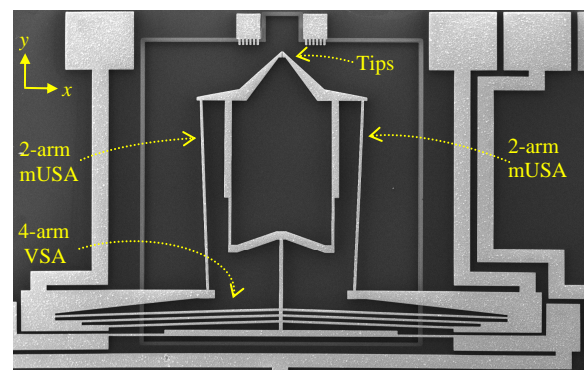


Figure 1: SEM image of a fabricated metallic MEMS gripper with structural configuration illustrated.

compared to a straight connection (in the structure known as Guckel or U-shape actuator - USA), the uniqueness of the mUSA is the connection of the hot arms, denoted by “ h_i ” (with $i = 1, 2, 3$), to the central joint beam with an angle of $90^\circ - \theta$. Based on simulations, an optimized angle of $\theta = 5^\circ$ is selected. The non-perpendicular jointing not only guarantees the desired in-plane directional displacement but also increases the traveling distance and actuating force. This distinguishes the MEMS gripper from the others [6-9] where USAs are used in the gripping mechanism.

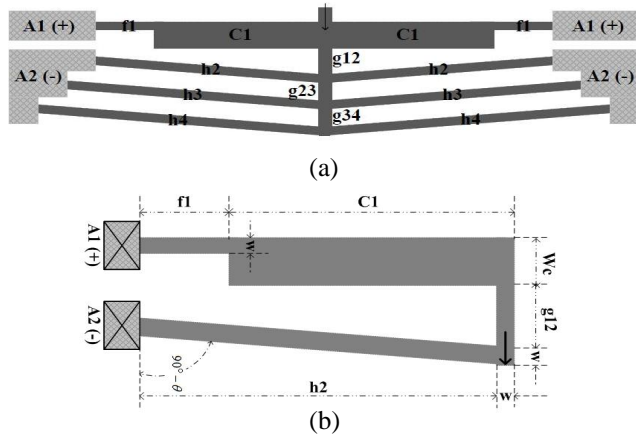


Figure 2: (a) A 4-arm V-shape Actuator (VSA), (b) a 2-arm Modified U-shape Actuator (mUSA).

It should be noted that the symmetric VSA in Fig. 2(a) can be considered as the combination of two 4-arm mUSAs that are uniquely integrated, or the combination of chevron beam actuators with unequal length and mUSAs. The flexure-cold arm labeled as $f1$ and $C1$ has two functions, i.e. to minimize the out-of-plane displacement of the chevron hot beams, and to reinitialize their displacement as a spring when the structures are de-actuated. In our VSA, due to the small cross sectional expansions, the focus is on one-dimensional analysis in which only the length changes of the structural beams are considered. The in-plane displacement of the actuator tip ΔY resulted from length expansions of the actuator beams is analyzed and discussed in [2-3] with polysilicon structures. Yet, the analytical models for the displacement and force F_v discussed in these papers are also valid for the nickel VSA in this MEMS gripper. Upon actuation of the VSA, the lengths of clamped-clamped chevron beams ($h_i - h_i$, with $i = 2, 3, 4$) shown in Fig. 2(a) expand to $\ell = L + \Delta L$. Consequently, a y-direction displacement ΔY at the central beam is generated, i.e.

$$\Delta Y_{vsa}(\ell) = \left(\frac{\ell}{2}\right) \cdot \sin \left[\cos^{-1} \left(\frac{L \cdot \cos(\theta)}{\ell} \right) \right] - \frac{L \cdot \sin(\theta)}{2} = \left(\frac{\Delta L}{2}\right) \cdot \sin(\theta) \quad (1)$$

As shown in Fig. 1, the VSA displacement ΔY and force F_v are applied to the two mUSAs to further drive the gripper tip opening. The mechanism is discussed in the following section.

3 GRIPPER OPERATION MECHANISM

Fig. 3 illustrates the 3D models of the electro-thermal MEMS gripper before and after actuation.

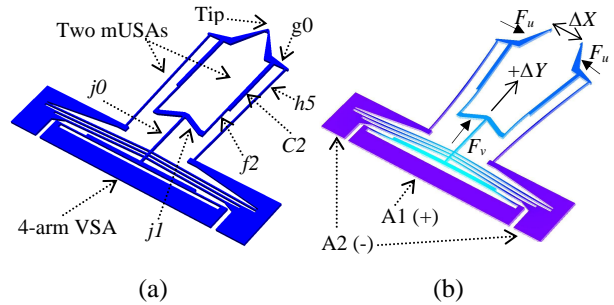


Figure 3: 3-D model of the gripper; (a) prior to actuation, and (b) after actuation.

In Fig. 2 (VSA) and Fig. 3 (gripper), $f1, f2, C1, C2, h2, h3, h4, h5, g34, g23, g12, j0, j1, g0$ denote the flexure, cold, hot, and joint beams, respectively. Upon actuating the gripper drivers, the y-direction in-plane force F_v and displacement ΔY_{vsa} generated by the VSA is transmitted to the mUSA beams $f2, C2, g0$, and ultimately $h5$ (fixed-end) via the central T-beam $j0$ and $j1$, resulting in mechanical bending forces at the $f2$ - $h5$ arm. Fig. 4 illustrates the gripper opening (mUSA displacement) due to the pushing force of the VSA. Simultaneously, the mUSA is energized to provide a thermal buckling force to bend the flexures $f2$ and $h5$ further. With joint forces from the VSA and the two mUSAs, this double actuation mechanism results in a larger gripper opening and holding force in x-direction.

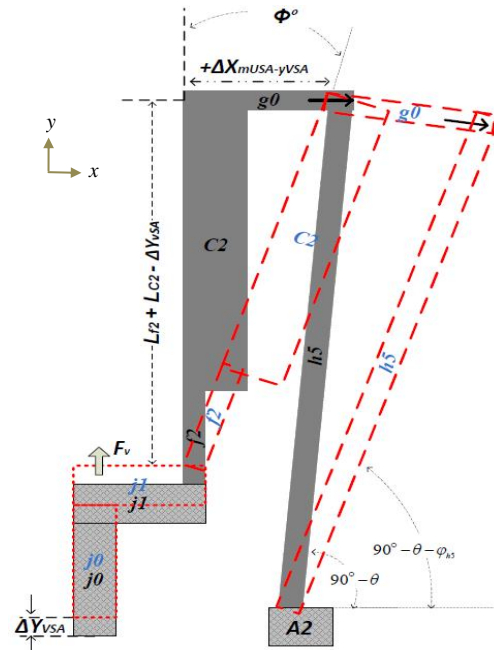


Figure 4: mUSA displacement; MEMS gripper opening due to mechanical pushing force of the VSA.

4 MODELING AND SIMULATION

The analytical modeling and simulation using MATLAB are conducted to optimize the design parameters and predict the behavior of the device. As shown in Fig. 5(a), the entire MEMS gripper can be modeled as a network of electro-thermal elements representing the beams in the gripper. A general lumped-element model of individual beams and consequently the entire device is presented in Fig. 5(b), in which R_e , R_T , C_T represents the electrical resistance, thermal resistance and thermal capacitance, respectively. In device modeling, the effect of temperature coefficient of resistance (TCR) of the beams is included. At a fixed voltage, total electrical current and power generated in the device is a direct function of the total resistance. The thickness of the electroplated nickel structure is $H=20\ \mu\text{m}$. The length by width dimensions $L \times W\ (\mu\text{m}^2)$ of the gripper structural beams are as; $f1=f2=250 \times 10$, $C1=C2=508 \times 25$, $h2=758 \times 10$, $h3=878 \times 10$, $h4=h5=998 \times 10$, $g34=g23=20 \times 15$, $g12=40 \times 15$, $j0=364 \times 15$, $j1=188 \times 40$, $g0=130 \times 25$. As presented in [2-3], the temperature distribution along the beam can be obtained by; $T(x) = (0.5 \cdot P_e \cdot \kappa^{-1}) \cdot (L \cdot x - x^2) + 300$ (K), where k is the thermal conductivity of the nickel. From the lumped model shown in Fig. 5, the average temperature within the structural beams can be obtained by,

$$T_R(t) = \frac{R_T}{R_{e0}} \cdot \left(\frac{V}{V_T}\right)^2 + (T_R(0) - \frac{R_T}{R_{e0}} \cdot \left(\frac{V}{V_T}\right)^2) \cdot \exp\left[-\left(\frac{V_T^2}{R_T \cdot C_T}\right) \cdot t\right] \quad (2)$$

where, the voltage change effect is $V_T = (1 + \alpha_r \cdot R_T \cdot R_{e0}^{-1} \cdot V^2)^{0.5}$.

The TCR of nickel, α_r , is experimentally measured as $0.004\ (\text{K}^{-1})$. As discussed in Section 3, the total gripper opening is attributed to both the y-displacement ΔY_{VSA} from the VSA and the x-displacement ΔX_{mUSA} from the two mUSAs. The opening ΔX_{mUSA} due to the thermal buckling displacement of the mUSA can be obtained from,

$$\Delta X_{mUSA} = (\ell_{h5}) \cdot \sin\left(\cos^{-1}\left(\frac{L_{h5} \cdot \cos(\theta)}{\ell_{h5}}\right)\right) - L_{h5} \cdot \sin(\theta) = \Delta L_{h5} \cdot \sin(\theta) \quad (3)$$

where, ℓ_{h5} , L_{h5} , ΔL_{h5} are the steady state, initial, and the change of the hot arm $h5$ length, respectively. With the force and displacement transfer mechanism illustrated in Fig. 4, the x-direction opening resulted from the pushing force from VSA can be expressed as,

$$\Delta X_{mUSA-yVSA} = (\ell_{f2} + \ell_{C2} + \ell_{tip}) \cdot \sin\left[\cos^{-1}\left(1 - \frac{\Delta Y_{VSA}}{\ell_{f2} + \ell_{C2} + \ell_{tip}}\right)\right] \quad (4)$$

Using initial geometrical parameters given in above, the beam length change caused by the temperature change ΔT can be obtained by $\ell = L \cdot (1 + \alpha_T \cdot \Delta T)$, where the thermal expansion coefficient of nickel is $\alpha_T = 0.0064\ (\text{K}^{-1})$. Ultimately, the total gripper opening at the tip can be obtained by $\Delta X = \Delta X_{mUSA} + \Delta X_{mUSA-yVSA}$. The holding force of the gripper F_u can be derived based on the spring stiffness

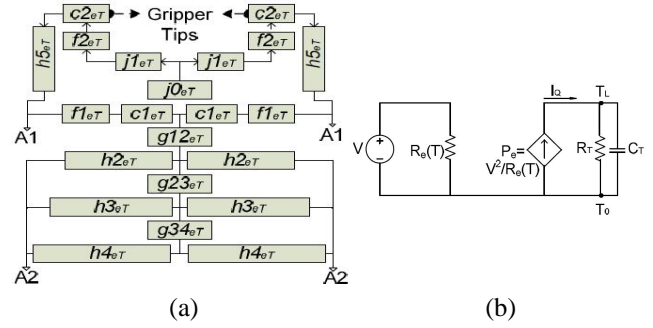


Figure 5: MEMS gripper models; (a) network of electro thermal elements, (b) lumped-element model of the structural beams or entire device.

of the mUSA and the total displacement of the gripper tip.

CoventorWare, a finite element analysis (FEA) tool dedicated for MEMS simulation has been used in design verification. Fig. 6 shows the simulated temperature distribution along the structural beams of the gripper. At 1.0V driving voltage, the maximum temperature of $\sim 470\ \text{K}$ occurs at the VSA cold arm $C1$. The gripper tip temperature remains below $396\ \text{K}$. The average operating temperature is $\sim 385\ \text{K}$. Also, at this 1 V operating voltage, in steady state, the VSA tip displacement is $\Delta Y \approx 22\ \mu\text{m}$ which results in the gripper tip opening of $\Delta X \approx 163\ \mu\text{m}$ with a gain of ~ 7.4 . The out-of-plane z-displacement maintains less than $0.01\ \mu\text{m}$, owing to the symmetric structural design. The VSA pushing force F_v and the mUSA holding force F_u are predicted as $\sim 8.6\ \text{mN}$ and $\sim 4.9\ \text{mN}$, respectively. The FEA results are in a good agreement with respective analytical results while both have shown reasonable predictions of the performance of the fabricated gripper.

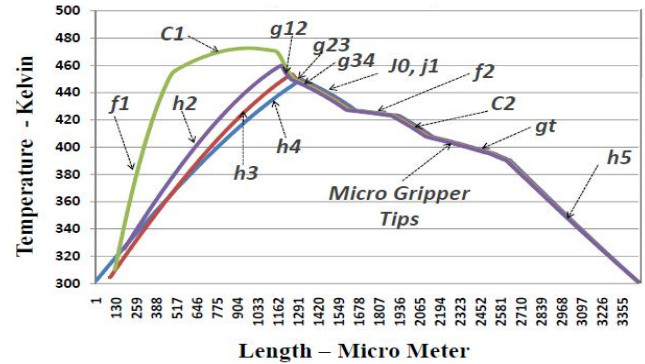


Figure 6: Temperature distribution within the beams of the gripper shown in Figures 1 and 3 at 1.0 V driving voltage.

5 DEVICE TESTS

Tests on the fabricated gripper and the actuators have shown attractive features. Fig. 7 shows a gripper in its actuated state, and the displacement profiles as functions of the actuation voltage. As the driving voltage ($V_{CC} = V_{AI(+)} - V_{AI(-)}$) varies within $0.6\sim 1.0\ \text{V}$, the loaded VSA

6 FABRICATION PROCESS

MetalMUMPs foundry service is employed for the device fabrication. A standard MetalMUMPs process [10] is used to fabricate the device shown in Fig. 1. The cross-sectional view of the fabricated device is illustrated in Figure 8. Electroplated nickel is used as structural material. To minimize the Joule heat radiated to the substrate, a 25 μm trench is etched underneath the gripper.

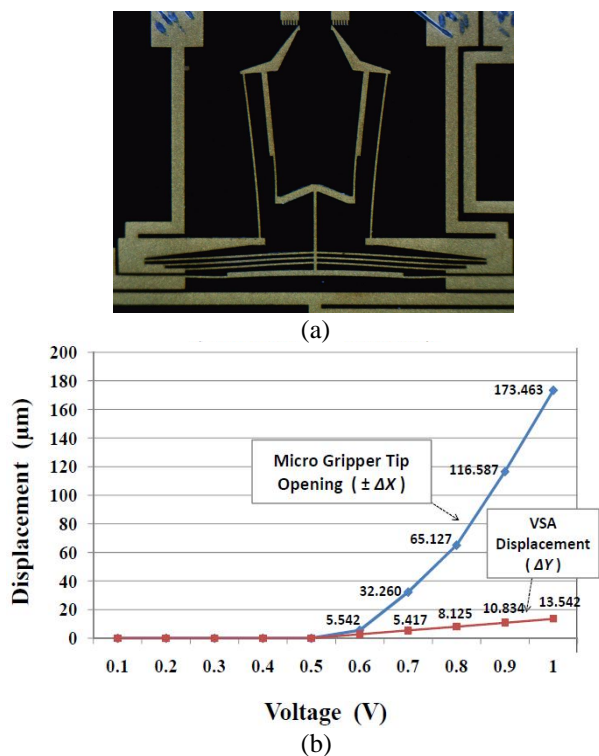


Figure 7: (a) Optical image of the micro gripper actuated at 1.0 V that generates a 173.4 μm opening; and (b) displacement response to voltage change; gripper opening versus VSA y -direction traveling distance.

parabolically generates in-plane displacements within $\Delta Y \approx 2.7\text{-}13.5 \mu\text{m}$ causing the gripper openings within $\Delta X \approx 5.5\text{-}173.5 \mu\text{m}$ (gain: $\sim 2\text{-}12.8$). The gripper opening sensitivity (dX/dV) alters within $\sim 0.27\text{-}0.57 \mu\text{m}/\text{mV}$. Although, the displacement response to temperature and voltage changes is nonlinear, but within $V_{cc}=0.6\text{-}1.0 \text{ V}$, the VSA displacement sensitivity (dY/dV) remains constant at $\sim 0.027 \mu\text{m}/\text{mV}$ indicating its controllability and linearity under the mechanical load as voltage changes. From $\sim 3.6 \mu\text{m}$ buckling of a spring test structure, the VSA pushing force F_v measured $\sim 8.4 \text{ mN}$ at $V_{cc}=1.0 \text{ V}$. The gripper average temperature is determined as 320-380 K within operating voltage of 0.6-1.0 V with consuming power of $\sim 0.34\text{-}0.85 \text{ W}$. More data are provided in Table 1.

Items	Micro Gripper Electro Thermo Mechanical Spec.		
	Description	4-arm VSA	2-arm mUSA
$L \times W \times H$	Size (μm^3)	2100 \times 140 \times 20	1050 \times 140 \times 20
R	Resistance (Ω)	1.0	1.5
T	Max. Temperature (K)	470	423
X -axis	Max. ΔX displacement (μm)	0.002	127.3 (tip: 173.5)
Y -axis	Max. ΔY displacement (μm)	13.5	16.25 (tip: 29.7)
Z -axis	Max. Z displacement (μm)	-0.006	0.013

Table 1: Major specifications of the metallic MEMES gripper at 1.0 V operating voltage.

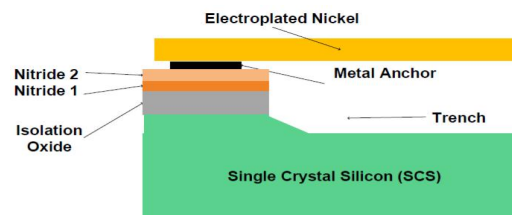


Figure 8: Cross-sectional view of the fabricated gripper.

7 CONCLUSIONS AND DISCUSSIONS

A metallic MEMS gripper has been successfully modeled, simulated and fabricated. Relatively, at a low operating voltage and power, the gripper average temperature stays low, and the VSA generates a large in-plane y -displacement causing a large gripper tip opening ΔX while the entire structure maintains very small out-of-plane z -displacements. Within the operating voltage, the gripper opening sensitivity (dX/dV) remains high and alters predictable. The VSA and mUSA designed in this gripper can also find applications in other associated MEMS devices.

REFERENCES

- [1] D. J. Bell, et al, *Journal of Micromechanics and Microengineering*, Vol. 15, 2005, pp.153-164.
- [2] J. J. Khazaai, et al, *2010 IEEE Sensors Conference*, 2010, pp. 1454.
- [3] J. J. Khazaai, et al, *2010 NSTI-Nanotech*, Vol. 2, 2010, pp. 681-684.
- [4] C. Kung, et al, *Journal of the Chinese Institute of Engineers*, Vol. 28, No. 1, 2005, pp. 123-130.
- [5] Q. Huang, et al, *Journal of Micromechanics and Microengineering*, Vol. 9, 1999, pp. 64-70.
- [6] K. Kim, et al, *Microsystem Technologies*, Vol. 10, 2004, pp. 689-693.
- [7] J. V. Crosby, et al, *the Proceedings of the COMSOL Conference*, 2009, Boston.
- [8] N. Chronis, et al, *Journal of Microelectro mechanical Systems*, Vol. 14, No. 4, 2005, pp. 857.
- [9] T. C. Duc, et al, *Journal of Microelectro mechanical Systems*, Vol. 17, No. 6, 2008, pp.1546.
- [10] MEMSCAP Inc., *MetalMUMPs Design Hand Book*, Revision 2.0.